Pattern formation of indirect excitons in coupled quantum wells

2006 J. Phys.: Condens. Matter 18 9659

(http://iopscience.iop.org/0953-8984/18/42/012)

INSTITUTE OF PHYSICS PUBLISHING JOURNAL OF PHYSICS: CONDENSED MATTER

J. Phys.: Condens. Matter **18** (2006) 9659–9668 doi:10.1088/0953-8984/18/42/012

Pattern formation of indirect excitons in coupled quantum wells

C S Liu[1,2], H G Luo[1] and W C Wu[2]

[1] Institute of Theoretical Physics and Interdisciplinary Center of Theoretical Studies, Chinese Academy of Sciences, PO Box 2735, Beijing 100080, People's Republic of China
[2] Department of Physics, National Taiwan Normal University, Taipei 11650, Taiwan

Received 2 August 2006, in final form 9 September 2006
Published 5 October 2006
Online at stacks.iop.org/JPhysCM/18/9659

Abstract

Using a nonlinear Schrödinger equation including short-range two-body attraction and three-body repulsion, we investigate the spatial distribution of indirect excitons in semiconductor coupled quantum wells. The results obtained can explain the experimental phenomenon that the annular exciton cloud first contracts then expands when the number of confined excitons is increased in the impurity potential well, as observed by Lai *et al* (2004 *Science* **303** 503). In particular, the model reconciles the patterns of exciton rings reported by Butov *et al* (2002 *Nature* **418** 751). At higher densities, the model predicts much richer patterns, which could be tested by future experiments.

(Some figures in this article are in colour only in the electronic version)

1. Introduction

Recently, great progress has been made on the research of exciton Bose–Einstein condensation (BEC) by making use of indirect excitons (spatially separated electron–hole pairs) in coupled quantum wells (CQWs). The advantage of the indirect excitons is that they have a long lifetime and a high cooling rate. With these merits, Butov *et al* have successfully cooled the trapped excitons to the order of 1 K [1]. Although there is not enough evidence to prove that the excitons are in the BEC state, it is interesting to observe several interesting photoluminescence (PL) patterns [2]. Independently, Snoke *et al* have also observed somewhat analogous PL patterns in a similar system [3]. The key features in the experiment of [2] are as follows. (i) Two exciton rings are formed. When a focused laser is used to excite the sample and the prompt luminescence is measured in the vicinity of the laser spot, a ring, called the internal ring, is formed, while a second ring of PL appears as distant as 1 mm away from the source, called the external ring. (ii) The intervening region between the internal and external rings is almost dark, except for some localized bright spots. (iii) Periodic bright spots appear in the external ring [2]. The bright spots follow the external ring either when the excitation spot is moved over

the sample, or when the ring radius is varied with the excited power. (iv) The PL is eventually washed out when the temperature is increased.

To explain the above features, a charge separated transportation mechanism was proposed which gives satisfactory results for the formation of the exciton ring and the dark region between the internal ring and external ring, and even the ring in a single quantum well [4, 5]. However, the physical origin for the periodic bright spots in the external ring is still controversial. It is commonly believed that the periodic bright spots are formed due to some kind of instability. Levitov *et al* considered that exciton states are highly degenerate and the instability comes from the stimulated scattering [6]. Sugakov suggested that the instability is due to the attractive interaction between the high-density excitons [7]. In addition, Yang *et al* proposed that the ring bright spots result from the interplay between the random potential and the nonlinear repulsive interaction of the condensed excitons [8].

More recently, great attention has been attracted by a surprising observation of trapped excitons in an impurity potential well. In the experiment of Lai *et al* [9], they used a defocused laser to excite CQWs in a large area. Excited electrons and holes are collected by an impurity potential well. The area of the defocused laser spot is typically larger than the area of the impurity potential well. The defocused laser spot can be applied either away from the impurity potential well or directly on it. It is found that the PL pattern is much more concentrated than a Gaussian with a central intensity dip, exhibiting an annular shape with a darker central region. In particular, on increasing the laser excitation power, the exciton cloud first contracts and then expands. Even more interestingly, on pumping by a higher-energy laser, the dip can turn into a tip at the centre of the annular cloud. In fact, this kind of annular shape pattern can also be found in some localized bright spots between the inner ring and external ring of Butov's experiment [2].

Neither the mechanism of stimulated scattering [6] nor the mechanism of pure attractive interaction between excitons [7] is able to explain the above remarkable phenomenon. With the mechanism of stimulated scattering, the stimulated scattering rate should enhance when the particle density is increased. Consequently, the annular ring should contract all the way and no expansion is expected. The mechanism of pure attractive interaction between excitons also has difficulty in explaining the expansion of excitons.

In this paper, we propose an alternative model to understand the formation of the bright spots in the exciton ring. We consider that the exciton system can be described by a nonlinear Schrödinger equation which includes attractive two-body and repulsive three-body interactions. The interplay between these interactions and the kinetic energy can lead to complex patterns, which are shown to be in great likeness to the experiments. The nonlinear Schrödinger equation is numerically solved and the corresponding spatial distribution of excitons not only can explain the ring bright spots but also can describe the contraction and the expansion phenomenon of the exciton ring. Some detailed features including a tip occurring at the centre of the annular cloud can also be reproduced. Our model predicts some new patterns at the higher-density regime, which can be tested by future experiments.

It is important to emphasize a key element which supports the proposed model. As pointed out in [4, 5], when electrons and holes are excited by a laser, they are hot electrons and hot holes initially. Since the drift speed of hot electrons is larger than that of hot holes (the electron has a smaller effective mass), electrons and holes are indeed charge separated. No true exciton is formed at this stage. Because hot electrons and holes have a small recombination rate, they can travel a long distance from the laser spot. After such long-distance travel, the hot electrons and holes collide with the lattice and are cooled down. The cooling speed of electrons is faster than that of holes, and consequently cooled electrons and cool holes will meet. This kind of charge-separated transportation mechanism has been used to interpret the exciton ring formation [4, 5].

In the experiment by Butov *et al* [2], they meet in the region of the (external) ring, while in the experiment by Lai *et al* [9], they meet in the impurity potential well. It is believed that cooled electrons and holes will form excitons. Thus the elemental particles in the external ring [2] and in the impurity potential well [9] are *excitons*. At this stage, the charges are not separated, but are coupled or bound together. They have long life. The interaction between excitons results in the nonhomogeneous density distribution which in turn results in the complex PL patterns. Since particles can only move in CQWs, their movements are basically two-dimensional. The PL intensity is directly proportional to the number of excitons. In the following discussion, we simply take the exciton probability density distribution as the PL distribution.

2. Remarks on interactions and equilibrium

There are two experimental facts which are important for the understanding of the pattern formation of the indirect excitons. (1) The distribution of the excitons is inhomogeneous and (2) the inhomogeneous distribution varies with the exciton number density. To understand these phenomena, the key may lie in the interactions between excitons. First, it is very clear that the interaction between the indirect excitons is neither purely attractive, nor purely repulsive. If the interaction between the indirect excitons is purely repulsive, it will drive the excitons towards a homogeneous distribution and the exciton cloud will expand with the increase of the number of excitons. At present there is no experimental signature to show this. On the other hand, if the interaction is purely attractive, the system is expected to collapse when the exciton density is greater than a critical value for which there is not enough kinetic energy to stabilize the exciton cloud. Experimentally the collapse of an exciton cloud has never been observed. In addition, the case of a purely repulsive or a purely attractive interaction is also against the experimental fact that the exciton cloud contracts first and expands later when the laser power is increased. The existence of the attractive interaction does not mean that the exciton state is unstable against the formation of metallic electron–hole droplet because the repulsive interaction may dominate over the attractive one in that regime.

Some remarks are in order on the existence of the attractive interaction. In contrast to the direct excitons in a bulk material or in a single quantum well, the indirect excitons have the same polarization direction since the indirect excitons are formed by electrons and holes which are spatially separated in different quantum wells. They are aligned dipoles. The interaction between the indirect excitons contains the dipole–dipole term and the van der Waals term [7]. The van der Waals attraction is given explicitly by the form $-C_6/r^6 - C_8/r^8 - \cdots$. When the spacing of the indirect excitons is large, the dipole–dipole interaction dominates, so the interaction is effectively repulsive. However, when the spacing of the indirect excitons becomes small, the van der Waals attraction will dominate the dipole–dipole interaction. It is found that the interaction becomes effectively attractive when the separation between two excitons is about 3–6 exciton radii [7]. In the current experiment, the exciton density is about 10^{10} cm^{-2}. For this density, the average distance between the indirect excitons is about 100 nm and the exciton Bohr radius a_B is about 10–50 nm [9], or the average distance between excitons is about 2–10 exciton radii. In such a case, it is reasonable to assume that the two-body interaction is in the attractive regime. In addition, when two indirect excitons approach each other, the exchange interaction between electrons becomes important, which also leads to an attractive interaction. In fact, the attractive interaction between the excitons has been considered as a possible candidate to describe the pattern formation observed by experiments [7, 10].

In the dilute limit, it is reasonable to assume that the free-energy density of the system is given by

$$F = F_0 + V_{ex}n - g_1n^2 + g_2n^3 + \cdots, \tag{1}$$

in terms of the expansion of exciton density n. Here F_0 is the free-energy density for hot electrons and hot holes (i.e., the case without a true exciton formed), $V_{\rm ex}$ is an external potential, and g_1 and g_2 are (positive) coupling constants associated with two-body and three-body interactions. The $-$ (+) sign with the g_1 (g_2) term denotes the attractive (repulsive) nature of the two-body (three-body) interaction. As elaborated above, the two-body interaction is believed to be effectively attractive in the system. Nevertheless inclusion of two-body interaction term only is not possible to give the system a better description (see later). If one keeps three-body terms in (1) as well, then it is necessary that the three-body interaction must be repulsive in order to keep the system stable. It will be shown soon that the inhomogeneous distribution of the exciton can be due to the competition between the two-body attraction and the three-body repulsion.

The interaction between excitons may be even more complex. It may include the Coulomb interaction (dipole–dipole interaction, van der Waals interaction) and exchange interaction. It may also include electron–phonon and Coulomb screening effects. In fact, we use two parameters g_1 and g_2 to describe all the above effects.

Another important issue is whether the excitons are in thermal equilibrium. If the excitons are all in the ground state, or a complete exciton BEC has been reached, their distribution must be Gaussian-like. The complex pattern observed in experiments indicates that this is not the case—quite a large number of excitons are in fact in excited states. Thus it is important to have a better knowledge of the energy distributions of the trapped excitons. The energy distribution in turn involves the (complex) energy relaxation and recombination processes, which have been studied by several experimental and theoretical groups [11]. For a relaxation process, when the exciton density is low ($n \ll a_{\rm B}^2$), the effects due to the exciton–exciton and the exciton–carrier scattering can be neglected. In this case, the relaxation time is mainly determined by the scattering of excitons off acoustic phonons [12]. In particular, at low bath temperatures ($T_{\rm b} < 1$ K), this kind of relaxation rate decreases dramatically due to the so-called 'phonon bottleneck' effects [11]. For the recombination process, because the excitons in the lowest self-trapped level are in a quantum degenerate state, they are dominated by the stimulated scattering when the occupation number is more than a critical value. Strong enhancement of the exciton scattering rate has been observed in the resonantly excited time-resolved PL experiment [13]. Therefore, even though the phonon scattering rate is still larger than the radiative recombination rate, thermal equilibrium of the system may not be reached. Essentially the distribution may deviate from the usual Bose one [14].

3. The model

To proceed with the above analysis, we use the following effective many-body Hamiltonian to describe the exciton system:

$$H = \int {\rm d}\mathbf{r}\, \psi^\dagger \left[-\frac{\hbar^2 \nabla^2}{2m^*} + V_{\rm ex}(\mathbf{r}) \right] \psi - \frac{g_1'}{2!} \int {\rm d}\mathbf{r}\, \psi^\dagger \psi^\dagger \psi \psi + \frac{g_2'}{3!} \int {\rm d}\mathbf{r}\, \psi^\dagger \psi^\dagger \psi^\dagger \psi \psi \psi, \qquad (2)$$

where $\psi^\dagger(\mathbf{r})$ [$\psi(\mathbf{r})$] denotes the creation (annihilation) of an exciton at the position $\mathbf{r}$, m^* is the effective mass of the exciton, and $V_{\rm ex}$ is the static external potential. g_1' is the coupling constant of two-body attraction, while g_2' is the coupling constant of three-body repulsion. In writing down the above Hamiltonian, the interactions between the excitons are assumed to be the contacted ones (i.e., the s-wave approximation is assumed). Under the mean-field approximation and neglecting the exciton-pair fields like $\langle \psi\psi \rangle$ and $\langle \psi^\dagger \psi^\dagger \rangle$ and the fields

involving any three operators, the mean-field Hamiltonian can be written as

$$H \approx \int \mathrm{d}\mathbf{r}\, \psi^\dagger \left[-\frac{\hbar^2\nabla^2}{2m^*} + V_{\mathrm{ex}} - g_1 n + g_2 n^2 \right] \psi, \tag{3}$$

where $n = n(\mathbf{r}) \equiv \langle \psi^\dagger \psi \rangle$ is the local density of excitons at $\mathbf{r}$, $g_1 \equiv 2g_1'$, and $g_2 \equiv 9g_2'$. The corresponding static *nonlinear* Schrödinger equation reads

$$-\frac{\hbar^2}{2m^*}\nabla^2\psi_j + (V_{\mathrm{ex}} - g_1 n + g_2 n^2)\psi_j = E_j \psi_j, \tag{4}$$

where ψ_j and E_j are the jth eigenstate and eigenvalue, respectively. It is assumed that the system is in a *quasi-equilibrium* state, and the spatial distribution of excitons is given by

$$n(\mathbf{r}) = \sum_{j=1}^{\mathcal{N}} \eta_j(E_j)|\psi_j(\mathbf{r})|^2, \tag{5}$$

where $\mathcal{N}$ denotes the total number of energy states that are *trapped* and η_j is an appropriate probability function associated with the energy level E_j. As a further assumption, we take

$$\eta_j \equiv \frac{\mathrm{e}^{-\beta E_j}}{\sum_{j=1}^{\mathcal{N}} \mathrm{e}^{-\beta E_j}}, \tag{6}$$

which has the form of Boltzmann distribution. Here β is a parameter used to describe the exciton distribution. The distribution (6) plays a central role in the calculation, which is shown to lead to qualitatively good results in agreement with experiments. Other possibilities have been tested, but none of them work.

Numerically it is convenient to first do the following scaling: $\psi_j(\mathbf{r})/\sqrt{N} \to \psi_j(\mathbf{r})$, $Ng_1 \to g_1$, and $N^2 g_2 \to g_2$, such that equation (4) retains the same appearance. In this case, $n(\mathbf{r})$ becomes the probability density which satisfies the normalization condition $\int_S n(\mathbf{r})\,\mathrm{d}S = 1$. Next, if we rescale $\psi_j(\mathbf{r})\sigma_{\mathrm{PL}} \to \psi_j(\mathbf{r})$ and $\mathbf{r}/\sigma_{\mathrm{PL}} \to \mathbf{r}$, equation(4) then reduces to

$$-\tfrac{1}{2}\nabla^2\psi_j + (v_{\mathrm{ex}} - a_1 n + a_2 n^2)\psi_j = \varepsilon_j \psi_j, \tag{7}$$

where $v_{\mathrm{ex}} \equiv V_{\mathrm{ex}}/\epsilon$, $a_1 \equiv g_1/(\sigma_{\mathrm{PL}}^2\epsilon)$, $a_2 \equiv g_2/(\sigma_{\mathrm{PL}}^4\epsilon)$, and $\varepsilon_j \equiv E_j/\epsilon$. Here $\epsilon \equiv \hbar^2/m^*\sigma_{\mathrm{PL}}^2$, with σ_{PL} being chosen by the root-mean-square radius of the exciton cloud observed by photoluminescence. With the above scaling, it is found that $a_1^2/a_2 = g_1^2/g_2\epsilon = g_1^2 m^*\sigma_{\mathrm{PL}}^2/g_2\hbar^2$, which is a constant for a particular sample. In the following, we shall use two different values of a_1^2/a_2 for the experiments by Lai *et al* [9] and by Butov *et al* [2].

In connection with real experiments, three important points should be clarified. (i) The exciton patterns are fully determined by its self-trapped interaction. The external potential V_{ex} is not the main cause for complex exciton patterns. In the experiment by Lai *et al* [9], the role of the impurity potential well is to collect the hot particles (electrons and holes) that form excitons. Thus we include a parabolic potential v_{ex} for calculations in regard to this experiment. However, in the experiment by Butov *et al* [2], the ring distribution of excitons is due to a charge separated transportation mechanism. It is believed that the size of the exciton ring is much larger than that of the impurity potential. So we will set $v_{\mathrm{ex}} = 0$ for calculations in regard to this experiment. (ii) When an electron and a hole form an exciton, it is believed that the kinetic energy is very low. This means that all the excitons are self-trapped in their self-trapped potential. A particle with energy above the self-trapped potential energy is not in the self-trapped well, and thus we should not take this kind of particle into account. (iii) We consider the excitons to be distributed initially in a Gaussian form. All self-trapped eigenstates ψ_j (i.e. $\varepsilon_j < 0$) along with $n(x, y)$ (via equation (5)) are then calculated self-consistently.

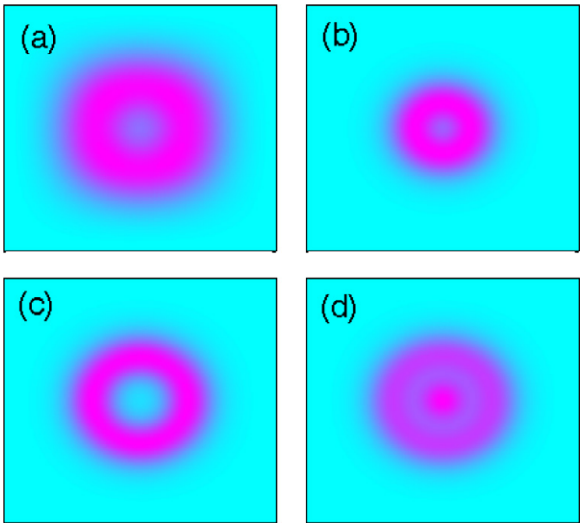

Figure 1. Formation of the annular distribution of the self-trapped excitons as a function of exciton number (a) $a_1 = 15$, (b) $a_1 = 25$, (c) $a_1 = 40$, (d) $a_1 = 55$ with $\beta = 0.0001$ in units of $1/\epsilon$ and $a_2 = 0.005a_1^2$. The results are intended to be compared with the experiment by Lai *et al* [9].

4. Results and discussions

4.1. Excitons in impurity potential well

Figure 1 shows the local probability density distribution $n(x, y)$ of the self-trapped excitons in an impurity potential well for four different particle numbers $a_1 = 15$, 25, 40, and 55. It is natural to quote the particle number N by a_1 since $a_1 \propto g_1$ with g_1 being rescaled to be $\propto N$. The impurity potential is taken to be parabolic,

$$v_{\rm ex}(\mathbf{r}) = \begin{cases} -0.8\,(r/\sigma_{\rm PL} - 1)^2 & \text{for } r \leqslant \sigma_{\rm PL}, \\ 0 & \text{otherwise}, \end{cases} \tag{8}$$

with a cutoff in simulating the real system. The plots are on a 2D plane and the colour scale denotes the relative amplitude of the local density $n(x, y)$. When the irradiating laser power is low (therefore, the self-trapped particle number is low), the dilute exciton cloud is diffused because the attractive interaction (g_1) is weak. When the laser power is increased (therefore, g_1 increases), stronger and stronger attraction drives the exciton cloud to shrink. When the particle number is further increased, the repulsive interaction (g_2) becomes more important, and eventually dominates over the attractive interaction. As a consequence, the exciton cloud expands again. The evolution of the exciton cloud with the exciton number (the laser power) is in good agreement with the experimental observation by Lai *et al* [9].

For a better illustration, the corresponding wavefunctions of the discrete energy levels related to figure 1(d) are plotted in figure 2. The wavefunctions related to the distributions in figures 1(a)–(c) are similar to those in figure 2. When the particle number is small (figure 1(a)), the number of self-trapped energy eigenstates involved is lower. The probability density distribution n is mainly determined by the superposition of the ground state and the first excited states. The ground-state wavefunction is an s-wave with a peak at the centre (see the wavefunction in figure 2(a)), while the first excited states are a nearly twofold degenerate p wave with a node at the centre (see the wavefunctions in figures 2(b) and (c)). Superposition

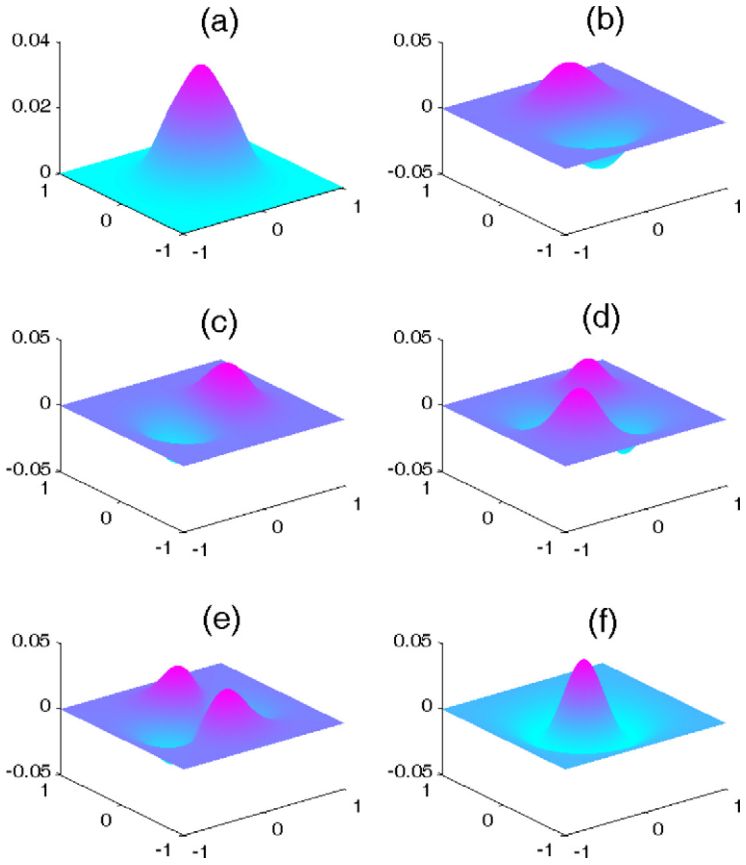

Figure 2. The corresponding lower-energy wavefunctions $z = \psi_i(x, y)$ related to the case of figure 1(d).

of these two states then lead to an annular distribution with a dip in the centre. With increasing particle number (figures 1(b) and (c)), the number of self-trapped energy eigenstates involved increases and the second excited states start to intervene. Second excited states are twofold degenerate d waves (see figures 2(d) and (e)). Thus a ring with much higher contrast is obtained. On further increasing the particle number, the third excited state (see figure 2(f)) then starts to intervene in the system. The superposition results in an annual distribution with a tip at the centre.

It is useful to estimate the values of g_1 and g_2 with respect to the real system. Taking figure 1(b) as an example, it is estimated that $n \approx 3.0 \times 10^{10}$ cm^{-2}. Since the experiment gives the root-mean-square radius $\sigma_{\mathrm{PL}} = 10\ \mu$m, the trapped exciton number $N = \pi\sigma_{\mathrm{PL}}^2 n \approx 9.4 \times 10^4$. One then obtains

$$g_1 = \frac{\hbar^2 a_1}{m^* \sigma_{\mathrm{PL}}^2 N} \times \sigma_{\mathrm{PL}}^2 \approx 4.93 \times 10^{-20}\ \mathrm{meV} \tag{9}$$

and

$$g_2 = \frac{\hbar^2 a_2}{m^* \sigma_{\mathrm{PL}}^2 N^2} \times \sigma_{\mathrm{PL}}^4 \approx 6.54 \times 10^{-36}\ \mathrm{meV}. \tag{10}$$

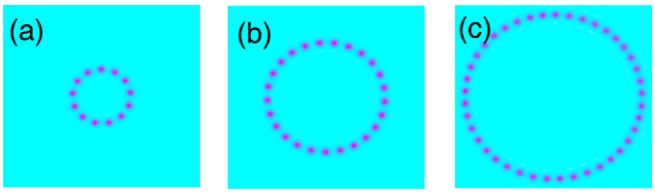

Figure 3. The formation of the bright ring spots for different exciton numbers: (a) $a_1 = 80$, (b) $a_1 = 150$, and (c) $a_1 = 250$. $\beta = 10^{-5}$ and $a_2 = 10^{-5}a_1^2$. The results are intended to be compared with the experiment by Butov *et al* [2].

Besides, if one assumes that the attractive interaction comes from an s-wave scattering, then the s-wave scattering length

$$a = \frac{a_1}{4\pi N} \approx 2.1 \times 10^4 \text{ nm}. \tag{11}$$

Moreover, since the exciton Bohr radius $a_B = 10$–50 nm, the ratio $a/a_B = 400$–2000. If we assume $\beta \equiv 1/k_B T$, the exciton temperature

$$T = \frac{\hbar^2}{m^* \sigma_{PL}^2 k_B \beta} \approx 0.2 \text{ K}. \tag{12}$$

4.2. Fragmented exciton ring

The same physical picture can also be employed to explain the ring bright spots observed by Butov *et al* [2]. In the present case, the exciton ring has formed with the charge-separated mechanism [4, 5]. The initial distribution of excitons is assumed to be homogenous in the ring. Considering that $\sigma_{PL} \sim 50$ μm, which is about five times larger than that in figure 1, the parameter a_1 is approximately 25 times larger than in the impurity potential well case. Figures 3(a)–(c) show the formation of the bright ring spots for different exciton numbers and ring radii (the exciton density was kept as a constant). On increasing the exciton number, the ring radii (an so the number of spots) increases, but the density of the bright spots remains unchanged. The periodic spots and the change of the spot number with exciton number (or laser power) are in qualitative consistence with the experimental observations [2]. In a real sample, non-homogeneity and some impurity may exist in the system. It is believed that the distorted and nonhomogeneous patterns are a result of the impurity potential. To give a better fitting to the experimental results, the external potential V_{ex} should be restored in the Schrödinger equation (4).

According to our picture, the physical origin of the bright ring spots is the consequence of the competition between the two-body attractive and three-body repulsive interactions and the kinetic energy. If excitons are uniformly distributed on the external ring initially, the attractive interaction will drive the excitons to move together. When the local density reaches a certain value, kinetic energy will drive the high-density excitons to diffuse. At the same time, the repulsive interaction also hinders further increasing of the exciton density. The competitive consequence leads to the formation of a series of clusters on the external ring. The size of these cluster is determined by the ratio of these three effects.

4.3. High-density patterns

The above calculations indicate that the phenomenological Schrödinger equation (4) gives a good description of the exciton distribution, both in an impurity potential well and in the

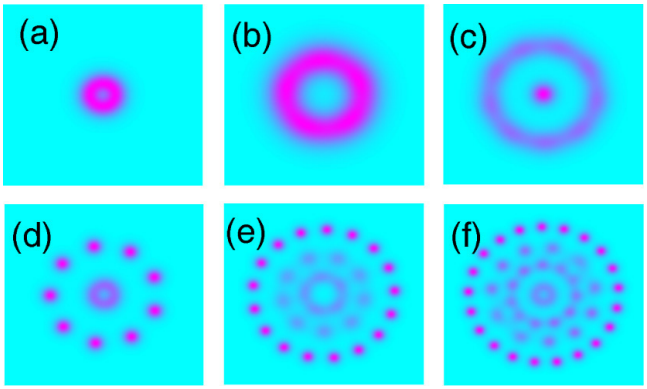

Figure 4. The density distribution for different exciton numbers: a_1 = (a) 20, (b) 30, (c) 60, (d) 80, (e) 200, (f) 300. Other parameters are the same as those in figure 2.

external ring. One open question is what will happen when the particle number in an impurity potential well is increased further. Figure 4 shows the numerical results for various exciton densities. When the exciton density is low (figure 4(a)), an annular distribution is observed. On increasing the density of excitons, the annular exciton cloud expands and a tip emerges at its centre (figures 4(b) and (c)). This phenomenon has been observed in the experiment by Lai *et al* [9]. When the density is increased further, the annular exciton cloud is unstable and a series of clusters form (figure 4(d)). In the case that the density is high enough, the competition between different interactions can in fact lead to very complex patterns beyond the present experimental observations. The clusters eventually form a pattern of a triangular lattice (figures 4(e) and (f)). We point out that all these patterns could be observable under current experimental conditions when the density is large enough.

5. Conclusion

Finally, some remarks are in order on the temperature effect. When the bath temperature is low, excitons are cooled and have relatively low momenta. The self-trapped interaction can confine most of the excitons. However, in the low momentum case, the cooling efficiency is low while the luminous efficiency is high, and excitons cannot reach the thermal equilibrium state. Due to the competition between the self-trapped and kinetic energies, complex exciton patterns occur (as discussed above). When the temperature is increased, the excitons are not fully cooled and correspondingly self-trapped interaction confines only some of the excitons. The attractive interaction cannot compensate the exciton kinetic energy and the excitons will distribute homogeneously in a 2D plane. In this case, the pattern is washed out. If the temperature is higher than the indirect exciton binding energy $\sim$3.5 meV [15, 16], most of the excitons become ionized and are in a plasma state. No pattern can be observed in this case. In order to realize exciton BEC, further experimental work should look for an effective method to obtain excitons with low combination rate and short relaxation time. The further theoretical work should be focused on the exciton interaction beyond the mean field approximation.

To summarize, we have demonstrated that the exciton distributions observed in experiments can be explained by the competition between the self-trapped interaction and the kinetic energy. A nonlinear Schrödinger equation including short-range two-body attractive and three-body repulsive interactions is used to describe the exciton behaviour. The interplay

among the two-body interaction, the three-body interaction, and the kinetic energy not only explains the experimental observations, but also leads to rich patterns, which could be tested in future experiments.

Acknowledgments

We acknowledge fruitful discussions with T Xiang, L Yu, Z B Su, G H Ji and J H Yuan. This work was supported by the National Natural Science Foundation of China (Grant No 10347149), National Basic Research Program of China (Grant No 2005CB32170X), and National Science Council of Taiwan (Grant No 93-2112-M-003-015).

References

[1] Butov L V, Lai C W, Ivanov A L, Gossard A C and Chemla D S 2002 *Nature* **417** 47
[2] Butov L V, Gossard A C and Chemla D S 2002 *Nature* **418** 751
[3] Snoke D, Denev S, Liu Y, Pfeiffer L and West K 2002 *Nature* **418** 754
[4] Butov L V, Levitov L S, Mintsev A V, Simons B D, Gossard A C and Chemla D S 2004 *Phys. Rev. Lett.* **92** 117404
[5] Rapaport R, Chen G, Snoke D, Simon S H, Pfeiffer L, West K, Liu Y and Denev S 2004 *Phys. Rev. Lett.* **92** 117405
[6] Levitov L S, Simons B D and Butov L V 2005 *Phys. Rev. Lett.* **94** 176404
[7] Sugakov V I 2004 *Preprint* cond-mat/0407398
[8] Yang S-R E, Park Q-H and Yeo J 2003 *Preprint* cond-mat/0312354
[9] Lai C W, Zoch J, Gossard A C and Chemla D S 2004 *Science* **303** 503
[10] Levitov L S, Simons B D and Butov L V 2005 *Solid State Commun.* **134** 51
[11] Benisty H, Sotomayor-Torrès C M and Weisbuch C 1991 *Phys. Rev.* B **44** 10945
[12] Piermarocchi C, Tassone F, Savona V, Quattropani A and Schwendimann P 1996 *Phys. Rev.* B **53** 15834
[13] Butov L V, Ivanov A L, Imamoglu A, Littlewood P B, Shashkin A A, Dolgopolov V T, Campman K L and Gossard A C 2001 *Phys. Rev. Lett.* **86** 5608
[14] Ivanov A L, Littlewood P B and Haug H 1999 *Phys. Rev.* B **59** 5032
[15] Snoke D W, Liu Y, Vörös Z, Pfeiffer L and West K 2005 *Solid State Commun.* **134** 37
[16] Szymanska M H and Littlewood P B 2003 *Phys. Rev.* B **67** 193305